Bioorganic & Medicinal Chemistry 20 (2012) 4693–4700

Contents lists available at SciVerse ScienceDirect

Bioorganic & Medicinal Chemistry

journal homepage: www.elsevier.com/locate/bmc

Synthesis, cytotoxic activities and cell cycle arrest profiles of half-sandwich *N*-sulfonamide based dithio-*o*-carborane metal complexes

Huan Dou [a], Wei Zhong [b], Liu Yang [a], Tingting Wang [a], Hong Yan [b,*], Yayi Hou [a,*]

[a] Immunology and Reproductive Biology Lab and Jiangsu Key Laboratory of Molecular Medicine, Medical School, Nanjing University, Nanjing 210093, China
[b] State Key Laboratory of Coordination Chemistry, School of Chemistry and Chemical Engineering, Nanjing University, Nanjing 210093, China

ARTICLE INFO

Article history:
Received 20 April 2012
Revised 4 June 2012
Accepted 5 June 2012
Available online 15 June 2012

Keywords:
Half-sandwich complex
Carborane
Non-small cell lung cancer
Apoptosis
Cell cycle arrested

ABSTRACT

Two half-sandwich cobalt and rhodium complexes **2a** and **2b** with combination of carborane and *N*-Sulfonamide were synthesized and fully characterized by NMR spectroscopy, mass spectrometry, elemental analysis as well as X-ray crystallography. In an in vitro cytotoxicity assay toward the non-small cell lung cancer cell lines of A549 and NCI-H460, **2b** showed the stronger activity than **2a**, which was confirmed by the morphological test. Mechanistic studies for **2b** showed that inhibition of NSCLC cell growth was mediated by G0/G1 cell cycle arrested without the significant apoptosis induction. Furthermore, **2b** altered the mRNA levels of *CCND1*, *CCNE1* and PCNA, which were known to control G0/G1 phase of the cell cycle. Our western blot analysis also showed that **2b**-induced G0/G1 cell cycle arrest was mediated through the decreased expression of cyclin D1, cyclin E1 and PCNA.

1. Introduction

Lung cancer is the most common cancer with high mortality throughout the world. In China it is the top of 10 malignant neoplasms.[1] Similarly, lung cancer is by far the leading cause of cancer death among both men and women in the United States, which will be an estimated 160,340 deaths in 2012 accounting for about 28% of all cancer deaths.[2] Of these, non-small cell lung cancer (NSCLC) accounted for ~85%.[3] Lung carcinoma is the result of molecular changes in the cell, resulting in the deregulation of pathways controlling normal cellular growth, differentiation, and apoptosis. The cell cycle is involved in these cellular processes, which is crucial to tumorigenesis. Cell cycle progression required precise expression and activation of several cyclins and cyclin-dependent kinases (CDKs). Once activated, the cyclin/CDKs form complexes that initiate phosphorylation of other proteins and downstream cyclin/CDK complexes. Alterations in these proteins, which lead to failure of cell cycle arrest, may thus serve as markers of a more malignant phenotype. Accordingly, improper progression through the cell cycle results in genomic and chromosomal instability as well as in uncontrolled proliferation.[4]

On the other hand, Organometallic complexes offer enormous scope for the design of anticancer candidates due to the large diversity of structure, bonding modes and wide range of ligand substitution rates that are unique to them.[5,6] In particular, the bioinorganic chemistry of metallocenes and half-sandwich metal complexes (e.g. Ru, Os, Ir) is an excellent example to demonstrate the considerable achievements of metal-based chemotherapy.[6–9] However, there are very few reported studies on the biological activity of half-sandwich cobalt and rhodium complexes.[10] Meanwhile, carborane derivatives[11–13] and *N*-Sulfonamides[14,15] have been utilized extensively in boron neutron capture therapy (BNCT) and medicinal chemistry, respectively. But the conjugates between *N*-sulfonamide and carborane together with transition metal complex to design the chemotherapy agents are still never explored.

We are interested in exploring whether the combination of half-sandwich cobalt and rhodium complexes with some potential biologically active ligands would result in novel efficient chemotherapeutic agents against human diseases. In this contribution, we synthesized two half-sandwich cobalt and rhodium complexes $Cp^*Co(S_2C_2B_{10}H_{10})(OH)[NHSO_2(4\text{-}CH_3)C_6H_4]$ (**2a**) and $Cp^*Rh(S_2C_2B_{10}H_{10})[NSO_2(4\text{-}CH_3)C_6H_4]$ (**2b**), containing carborane and *N*-Sulfonamide, and examined the in vitro cytotoxicity and induction of apoptosis/cell cycle arrest by the half-sandwich cobalt and rhodium complexes treatment against A549 and H460cells.

2. Results and discussion

2.1. Chemistry

To introduce the *N*-sulfonamide ligand into $Cp^*M(E_2C_2B_{10}H_{10})$ framework with the consideration of medicinal effect, here we

Abbreviations: NSCLC, Non-small cell lung cancer; CDKs, cyclin-dependent kinases; BNCT, boron neutron capture therapy; PCNA, proliferating cell nuclear antigen.

* Corresponding authors. Tel./fax: +86 025 83686441.
E-mail addresses: hyan1965@nju.edu.cn (H. Yan), yayihou@nju.edu.cn (Y. Hou).

0968-0896/$ - see front matter © 2012 Elsevier Ltd. All rights reserved.
http://dx.doi.org/10.1016/j.bmc.2012.06.016

investigated the reactions of $Cp^*M(S_2C_2B_{10}H_{10})$ (M = Co, Rh) with *p*-toluenesulfonyl azide (TsN_3).

Treatment **1a** with excess TsN_3 at room temperature for 4 days gave **2a** in good yield (Scheme 1). Switching the reaction condition into refluxing dichloromethane, the reaction time shortens within 20 h. The formation of **2a** might undergo an intermediate **IT**, which supported by its analog isolated in the reaction of $CpCo[S_2C_2(COOMe)_2]$with TsN_3,[16] and then nucleophilic addition with the traces of H_2O presenting in 'so-called' dry system at Co–N bond occurred to give final product. Any efforts to isolate the intermediate **IT** just lead to failure. However, the MS data of the mixture of reaction solution strongly suggest the presence of the intermediate **IT**, showing a strong peak at *m/z* = 570.03, which is fitting the proposed formulation well. The fact that we cannot isolate intermediate **IT** might be attributed to the impact of steric effects of Cp^* ligand.

The analogous reaction of **1b** with TsN_3 was performed at room temperature for 24 h or in refluxing dichloromethane within 6 h. After workup by chromatography, complex **2b** was isolated in ~70% yield.

Both complexes **2a** and **2b** were characterized fully by NMR spectroscopy (^1H, ^{11}B, ^{13}C), mass spectrometry, elemental analysis as well as X-ray crystallography. ORTEP representations of **2a** and **2b** with selected bond distances and angles are shown in Figure 1. For **2a**, the molecular structure confirms the expected three-legged piano-stool geometry with one hydroxyl and two chelating sulfur atoms to complete the coordination sphere about the metal. The Co–S bond lengths are 2.234 and 2.255 Å, slightly longer than those in complex **1a** (Co–S, 2.145 and 2.106 Å).[17] All other distances and angles lie in the expected range. The ^1H NMR spectra show the Cp^*, Me and Phenyl at δ = 1.51, 2.40 and 7.21–7.70 ppm, respectively, as well as the resonances at δ = 1.69 and 7.82 ppm due to OH and NH groups. The ^{13}C NMR spectra show the expected number of C–H and quaternary carbons and particularly the signals assigned to carborane cage at δ = 96.08 and 100.19 ppm. For **2b**, the structure shows an unique five-membered metallacyclic ring Rh–S–N–S–O which is generated by one *p*-toluenesulfonyl azide insertion Rh–S bond with the loss of N_2, followed by sulfone coordination to metal. The distances of S3–N1(1.568(3) Å) is 0.076 Å shorter than S2–N1(1.643(3) Å) and the distances of S3–O1(1.479(3) Å) is 0.045 Å longer than S3–O2(1.434(3) Å). This phenomenon indicates that N1–S3–O1 is a conjugated $_3{}^4\pi$ system. NMR spectra show the Cp^*, Ts and carborane ligands in expected range.

2.2. Biological activity

To test the anticancer activities of the synthesized compounds, we first analysed the effects of various concentrations of complexes **2a** and **2b** on the proliferation of the human NSCLC cell lines A549 and H460 by CCK-8 assay. In A549 cells the treatment with increasing doses of **2a** and **2b** for 48 h caused a dose-dependent inhibition of cell proliferation (Fig. 2A left), with IC_{50} values of 47.94 ± 0.93 μM and 6.09 ± 1.28 μM, respectively. The proliferation of H460 cell line (Fig. 2A right) was also significantly reduced in a wide range of doses of **2a** and **2b**. And the IC_{50} of **2a** and **2b** against H460 cells were 15.03 ± 0.70 μM and 1.71 ± 0.03 μM, respectively. Since **2a** and **2b** were such novel metal complexes, we compared the potency for cytotoxic activity of these two compounds with cisplatin, a prototypical metal-based anticancer drug. Previous cytotoxicity studies have been reported that IC_{50} values of cisplatin in A549 and H460 cells were at a range of 18–40 μM and 2.8–6 μM, respectively.[18–26] In contrast to cisplatin, **2b** almost showed considerable enhanced cytotoxicities against the two NSCLC cells. Moreover, the data exhibited significant cytotoxic activities in the order of **2b** > **2a**, and we selected **2b** for further anticancer studies. Additionally, we observed the morphological changes of **2b** on A549 cells. After the cells were treated with different concentrations of **2b** for up to 48 h, the A549 cells reduced numbers, elongated, and dissociated in a dose-dependent manner (Fig. 2B).Thus indicated significant cytotoxic effect of **2b** in A549 cells. These results suggest that **2b** may have potent improved antiproliferative activity.

A549 cells were treated for 48 h with **2b** under the IC_{50} value, and then monitored for apoptosis and cell cycle progression related parameters (Fig. 3). We performed a biparametric cytofluorimetric analysis using PI and Annexin-VFITC to characterize the mode of cell death, which stain DNA and PS residues, respectively.[27] After the treatment with indicated concentrations of **2b** (0, 2 and 5 μM) for 48 h, A549 cells were labeled with the two dyes and washed, and the resulting red (PI) and green (FITC) fluorescence was monitored by flow cytometry. We observed the appearance of Annexin-V^+/PI $^-$cells, indicative of apoptosis, as shown in the representative histograms depicted in Figure 3A. Quantitatively, **2b** treatment (<IC_{50}) did not result in a significant induction of apoptotic cells after 48 h. As we could not detect any induced apoptosis effect of **2b** on A549 cells, we next studied its possible effect on the cell cycle, according to previous cytotoxic effect. **2b** treatment resulted in the accumulation of cells in the G0/G1 phase, with a concomitant reduction in the proportion of cells in the G2/M phase. A small decrease of cells in the

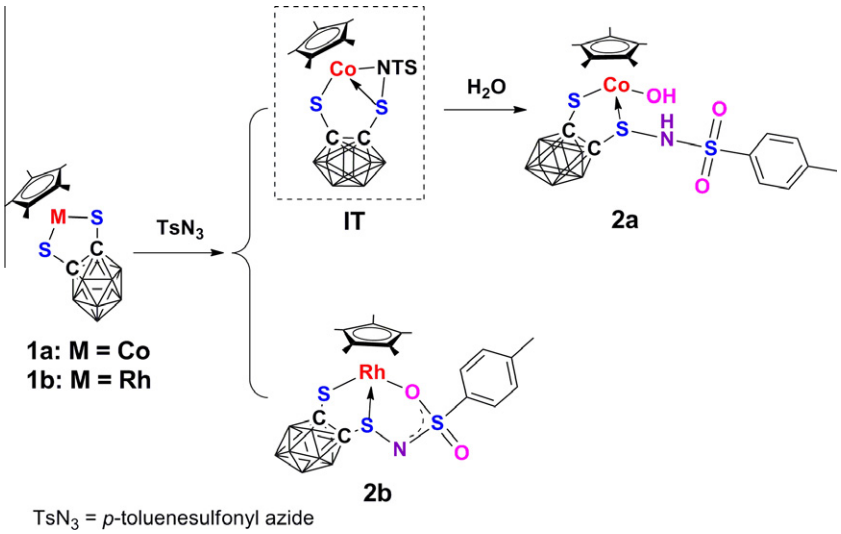

Scheme 1. The synthesis of complexes **2a** and **2b**.

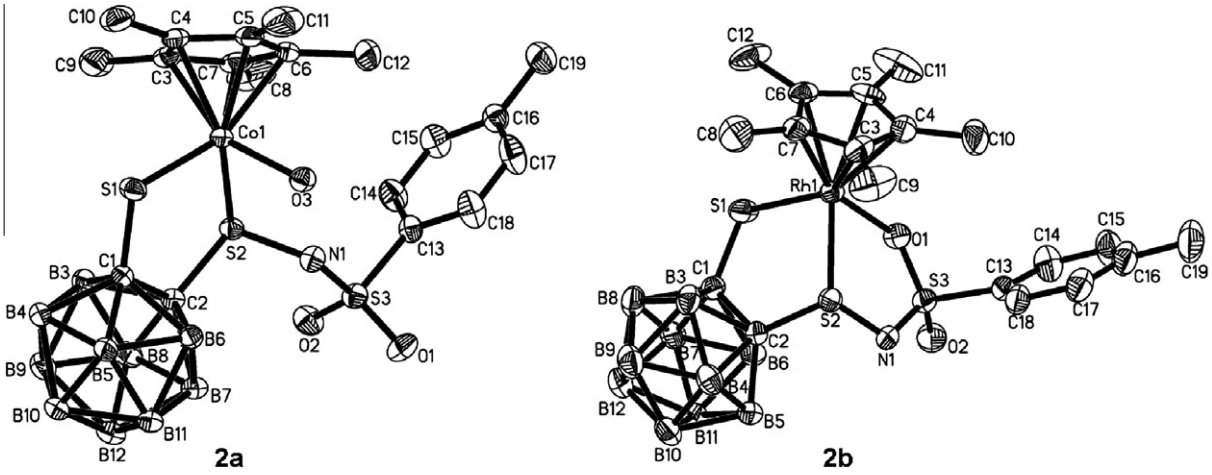

Figure 1. Molecular structures of **2a** and **2b** with 30% displacement ellipsoids. H atoms are omitted for clarity. Selected bond lengths (Å) and angles (°) for **2a**: Co1–S1 = 2.2340(9), Co1–S2 = 2.2552(10), Co1–O3 = 2.0136(16), S1–C1 = 1.775(3), S2–C2 = 1.826(2), S2–N1 = 1.645(2), C1–C2 = 1.664(4); S1–Co1–S2 = 94.11(3), S1–Co1–O3 = 96.77(6), S2–Co1–O3 = 89.46(7), Co1–S1–C1 = 106.11(9), Co1–S2–N1 = 102.21(9), Co1–S2–C2 = 105.65(11), N1–S2–C2 = 104.02(12), S1–C1–C2 = 118.48(17), S2–C2–C1 = 115.1(2). For **2b**: Rh1–S1 = 2.3520(15), Rh1–S2 = 2.3647(11), Rh1–O1 = 2.184(2), S1–C1 = 1.775(4), S2–C2 = 1.817(5), S2–N1 = 1.643(3), S3–O1 = 1.479(3), S3–O2 = 1.434(3), S3–N1 = 1.568(3), C1–C2 = 1.662(7); S1–Rh1–S2 = 91.08(4), S1–Rh1–O1 = 91.18(9), S2–Rh1–O1 = 79.64(7), Rh1–S1–C1 = 106.18(18), Rh1–S2–C2 = 104.79(14), Rh1–S2–N1 = 106.63(11), N1–S2–C2 = 104.01(16), O1–S3–N1 = 112.20(15), Rh1–O1–S3 = 120.66(16), S2–N1–S3 = 118.57(19), S1–C1–C2 = 118.2(3), S2–C2–C1 = 118.4(2).

S phase was also observed (Fig. 3B and C). The accumulation in G0/G1 cells was is concentration dependent. The characteristic hypodipolid peak (subG1), indicating apoptotic cells, did not appear until after 48 h of treatment (Fig. 3B), consistent with the apoptosis assay described above. According to various work from other labs, we compared the cell cycle profiles of cells subjected to **2b** and cisplatin, considering the similar micromolar range of cytotoxic activity for the A549 lung carcinoma cell line.[28–30] **2b** treatment of the A549 cells caused arrest at the G1-S boundary, while the cells treated with cisplatin maintained a significant increase in S phase or G2/M phase.[31]

To understand further the mechanism of cell cycle arrest induction by **2b**, we investigated the changes in the expression levels of transcripts encoded by genes associated with cell cycle at the G0/G1 phase, such as *CCND1* and *CCNE1*, by real-time quantitative PCR. Proliferating cell nuclear antigen (PCNA) is routinely used proliferation marker, which fulfils the requirements of molecular tumor markers to varying extents. A549 cells were treated with 10 μM **2b** for 6 h and 12 h, respectively, and the mRNA expressions of these three genes were markedly downregulated. The time-dependent response for inhibition of *CCND1*, *CCNE1* and PCNA is shown in Figure 4. **2b** down-regulated *CCND1*, *CCNE1* and PCNA mRNA significantly, indicating that **2b** could attenuate these gene expression at the transcriptional level. Expressions of cyclin D1 (*CCND1*), cyclin E1 (*CCNE1*) and PCNA were also investigated in the control and treated tumors by western blot analysis. As shown in Figure 5, we found that induction of the G0/G1 phase arrest was associated with the appreciable decreased expression of cyclin D1and cyclin E1, which have key roles in regulating the entry of cells at the G1/S transition checkpoint, and followed apparent decrease of PCNA in A549 cells, which is consistent with the previous cytotoxic assay.

Poor clinical survival rate has prompted the need for new therapeutic strategies for treatment of lung cancer. Currently the possibility to extend the BNCT technique to diffuse lung tumors is under investigation: complexes **2a** and **2b** were evaluated the potential in antitumor activity in vitro against NSCLC cells, and selected **2b** to elucidate mechanisms that contribute to the antitumor responses. This is the first study that demonstrated **2b** treatment against lung cancer. We have selected fast growing H460 and slow growing A549 cells to assess the antiproliferation effects of **2a** and **2b**. CCK-8 analysis showed that **2b** had stronger cytotoxicity in H460 and A549 NSCLC cells with IC_{50} value far less than 10 micromoles, and morphological changes were observed. To study the mechanism involved in the potent cytotoxicity of **2b**, we evaluated the induction of apoptosis and cell cycle progression in A549 cells after treatment for 48 h. Results indicated that no significant increasing trend in the apoptotic cell population can be observed for 48 h after **2b**, whilst cells are found to temporarily accumulate in the G0/G1 phase of the cell cycle. Many proteins are involved in this process and regulate accurate transition of the cell through subsequent phases of the cell cycle: G1, where cells grow in size, assess their metabolic status and prepare for division; S, where genome duplication occurs; G2, where cells check for completion of DNA replication and get ready to divide; and M, where mitosis takes place. Thus, we next focus on the key regulators on G0/G1 cell cycle arrest.

Our study has also revealed that high cyclin D1 and cyclin E1 expressions are significantly downregulated both at transcription and translation levels in A549 cells, suggesting the important roles of cyclin D1 and cyclin E1 in **2b** induced cell cycle arrest progression. Cyclin D1 serves as the regulatory subunit of CDK 4 and 6 and exhibits the ability to bind and sequester the CDK inhibitor p27.[32,33] Together, these functions facilitate cyclin-dependent kinase-mediated phosphorylating and inactivate the retinoblastoma protein and promote progression through the G1-S phase of the cell cycle. Moreover, cyclin D1 may regulate gene transcription through physical associations with a plethora of transcriptional factors, coactivators, and corepressors that govern histone acetylation and chromatin remodeling proteins.[32] Suppression of cyclin D1 expression has been shown to block tumorigenesis or to reverse the transformed phenotype of lung cancers in mice.[34] Cyclin E1 is also known as a positive regulator of G1-S transition, DNA replication and S-phase progression.[35,36] Cyclin E1-CDK2 complex phosphorylates and inactivates retinoblastoma protein, leading to the release of E2F, which in turn promotes S-phase entry. Cyclin E1 also has a critical role in the binding of MCM proteins to replication origins and in centrosome duplication. Additionally, high cyclin E1 expression promotes genetic instability and aneuploidy,[37,38] contributing to tumor progression by increasing genetic diversity among tumor cells.[39] In this study, we have identified the novel

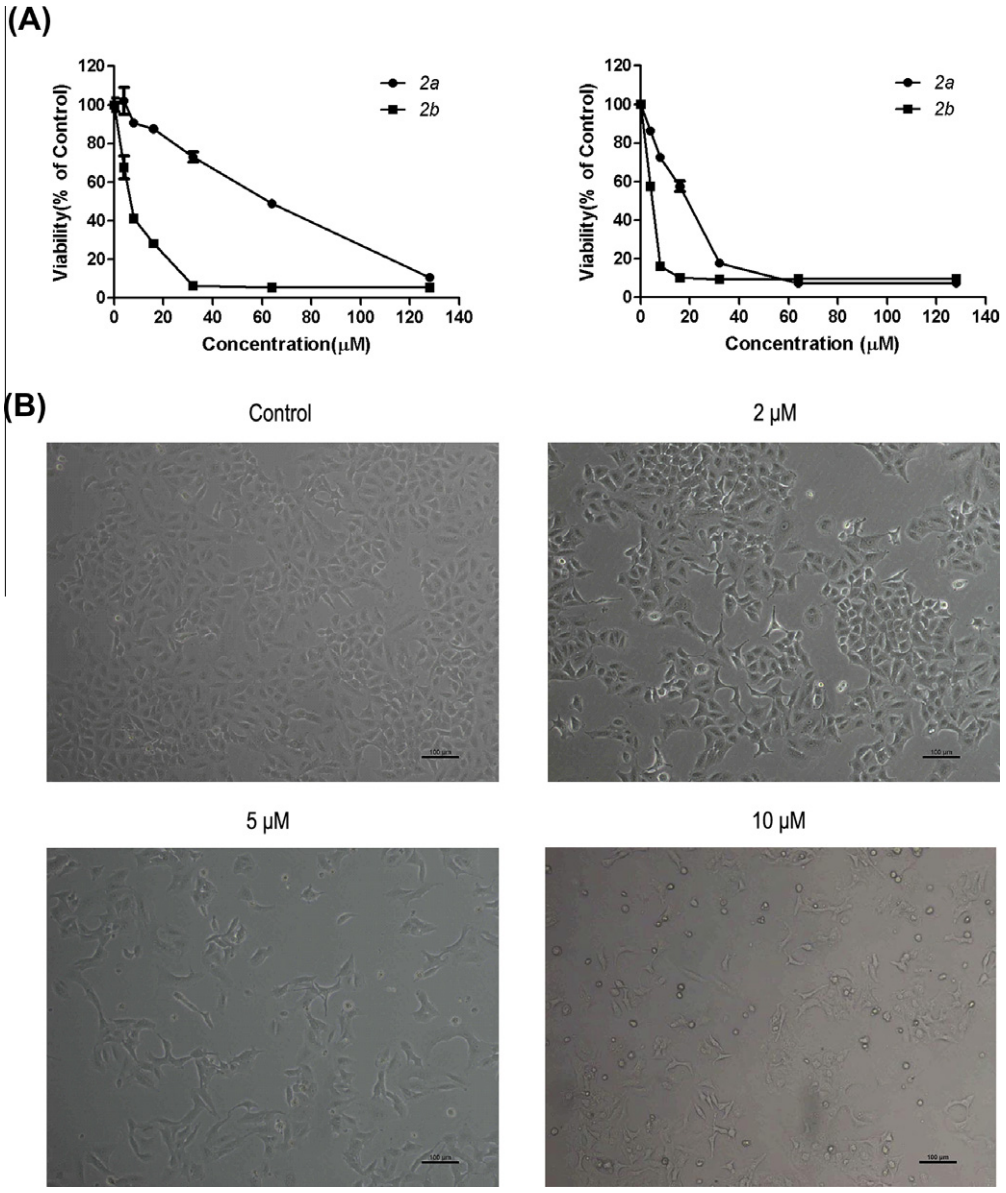

Figure 2. (A) Antiproliferation effect of **2a** and **2b** in A549 (Left) and H460 (Right) lung cancer cells. Cells were plated and incubated with indicated concentrations of **2a** and **2b** (0, 4, 8, 16, 32, 64 and 128 μM), after 48 h of incubation the viable cells were measured by CCK-8 assay. Data represent the means ± SEM of triplicate experiments. (B) Morphological changes of A549 after treatment with **2b** for 48 h. A549 cells were treated with vehicle (DMSO) or 2–10 μM **2b** for 48 h. Images under visible light were observed at 40× magnification. The results are representative of three independent experiments.

roles of cyclin D1 and cyclin E1 in the 2b-induced G0/G1 cell arrest of NSCLC cells, together with the validation of PCNA (the proliferation marker).

3. Conclusions

In summary, two new organometallic complexes **2a** and **2b** containing both *N*-sulfonamide and carborane skeleton have been synthesized from the reactions of 16*e* complexes **1a** and **1b** with *p*-toluenesulfonyl azide, respectively. Both complexes **2a** and **2b** inhibited the growth of the human NSCLC cell lines A549 and H460, but **2b** demonstrated more effective than **2a**. Furthermore, the growth inhibitory effect of **2b** could be associated to alterations in the cell cycle profile of A549 cells without an significant induction of cellular apoptosis. Both down regulating mRNA and protein levels of *CCND1*, *CCNE1* and PCNA, which were known to control G0/G1 phase of the cell cycle, validated the mechanism of **2b** at least in part. These findings provided a molecular basis for the pharmacological exploitation of **2b** to develop a novel class of organometallic complex containing *N*-sulfonamide and carborane skeleton for lung cancer therapy.

4. Experimental

4.1. Chemistry

4.1.1. General procedures

The starting material **1a**[40], **1b**[40] and *p*-toluenesulfonyl azide[41] were prepared according to literature. All reactions were carried out under argon using standard Schlenk techniques, unless otherwise stated. All solvents were dried and deoxygenated prior to use. Diethyl ether, tetrahydrofuran, and petroleum ether were refluxed and distilled over sodium/benzophenone under nitrogen. CH_2Cl_2 was distilled over CaH_2 under nitrogen. The NMR measurements were performed on a Bruker DRX 500 spectrometer. Chemical shifts were given with respect to $CHCl_3/CDCl_3$ (δ ^1H = 7.27 ppm; δ

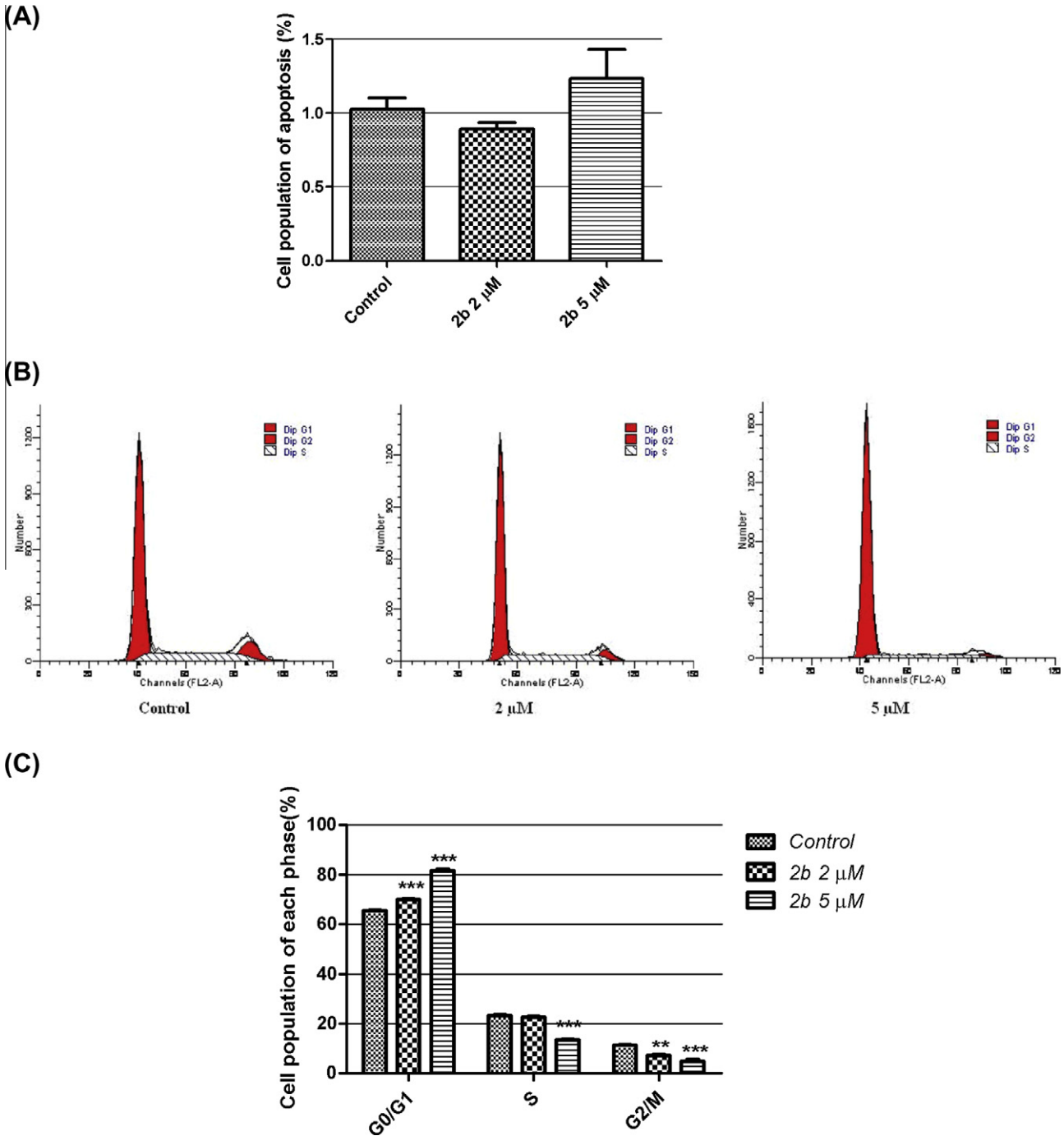

Figure 3. Effects on cell death and cell cycle of **2b**. A to C, A549 cells were treated with vehicle DMSO(Control), 2 μM or 5 μM **2b** for 48 h followed by cytofluorometric analysis of apoptosis-associated parameters (A) and DNA content (B and C). (A) The proportion of apoptosis cells (Annexin V-FITC$^+$/PI$^-$) were analyzed. (B) Representative cell cycle distributions of control versus **2b**-treated cells. (C) Cell populations in different phases were analyzed. Data points are mean values ± standard deviations of three separate experiments ($^{**}P$ <0.01 and $^{***}P$ <0.001, compared with control cells).

^{13}C = 77.0 ppm) and external $Et_2O{\cdot}BF_3$ ($\delta\,^{11}B$ = 0 ppm). The IR spectra were recorded on a Bruker Vector 22 spectrophotometer with KBr pellets in the region of 4000–400 cm^{-1}. The C, H and N microanalyses were carried out with an Elementar Vario EL III elemental analyzer. Mass data were determined with the LCQ (ESI-MS, Thermo Finnigan) mass spectrometer.

4.1.2. Preparation of 2a and 2b

Complex **1a** (81.0 mg, 0.2 mmol) or **1b** (89.0 mg, 0.2 mmol) was treated with *p*-toluenesulfonyl azide (197.3 mg, 1.0 mmol) at room temperature or under reflux in dichloromethane (20 mL) under a stream of Ar. The solvent was then removed under reduced pressure, and the residue obtained was dissolved in the minimum amount of dichloromethane for flash chromatographic separation on silica gel in a gradient eluting manner (petroleum ether/dichloromethane, 1:1, 1:5 and then dichloromethane/ethyl ether, 20:1) to give **2a** or **2b**.

2a (100.6 mg, 85.6%): green solid; ^{1}H NMR ($CDCl_3$, ppm): 7.83 (s, 1H, N*H*), 7.70 (d, *J* = 5.0 Hz, 2H, Ar*H*), 7.21 (d, *J* = 5.0 Hz, 2H, Ar*H*), 2.40 (s, 3H, CH_3), 1.67 (s, 1H, O*H*), 1.51 (s, 15H, Cp*); ^{11}B{^{1}H} NMR ($CDCl_3$, ppm): −2.1 (4B), −5.0 (2B), −6.4 (3B), −8.7 (1B); ^{13}C NMR ($CDCl_3$, ppm): 10.10 (CH_3, Cp*), 21.48 (CH_3), 95.88

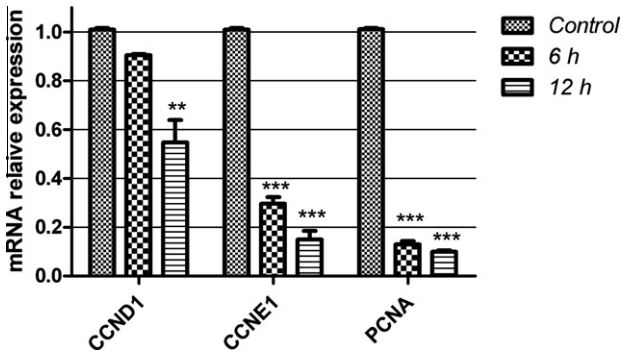

Figure 4. Effect of **2b** on the expression of cell cycle-related genes. Expression levels of *CCND1*, *CCNE1* and PCNA mRNA were determined by real-time quantitative PCR and expressed as relative fold expression to control. Data are shown as mean ± SEM of three independent experiments (**P <0.01 and ***P <0.001, compared with control cells).

(C, Cp*), 96.08 (carborane), 100.19 (carborane), 126.33 (CH, Ph), 127.81 (C, Ph), 129.01 (CH, Ph), 142.48 (C, Ph); ESI-MS (*m/z*): 571.08 (45%) $[M-H_2O+H]^+$, 590.11 (100%) $[M+H]^+$; elemental analysis calcd (%) for $C_{19}H_{34}B_{10}NO_3S_3Co$: C 38.83, H 5.83, N 2.38; found: C 39.06, H 5.71, N 2.17; IR (KBr, cm^{-1}): 2578.2 cm^{-1} (ν_{B-H}).

2b (110.4 mg, 70.5%): yellowish red solid; ^1H NMR ($CDCl_3$, ppm): 7.85 (d, J = 7.5 Hz, 2H, Ar*H*), 7.28 (d, J = 7.5 Hz, 2H, Ar*H*), 2.43 (s, 3H, CH_3), 1.79 (s, 15H, Cp*); $^{11}B\{^1H\}$ NMR ($CDCl_3$, ppm): −2.4 (4B), −5.9 (6B); ^{13}C NMR ($CDCl_3$, ppm): 9.67 (CH_3, Cp*), 21.51 (CH_3), 99.36 (carborane), 126.92 (C, Cp*), 129.19 (4 × CH, Ph), 129.68 (C, Ph), 142.87 (C, Ph); ESI-MS (*m/z*): 615.17 (40%) $[M+H]^+$, 1249.83 (100%) $[2M+Na]^+$; elemental analysis calcd (%) for $C_{19}H_{32}B_{10}NO_2S_3Rh$: C 37.19, H 5.26, N 2.28; found: C 37.33, H 5.09, N 2.11; IR (KBr, cm^{-1}): 2569.5 cm^{-1} (ν_{B-H}).

4.1.3. X-ray crystal structure determinations

Crystals suitable for X-ray analysis were obtained by slow evaporation of a solution in petroleum ether/dichloromethane. Diffraction data were collected on a Bruker SMART Apex II CCD diffractometer by means of graphitemonochromated Mo Kα (λ = 0.71073 Å) radiation at room temperature. The structures were solved by direct methods with the SHELXS-97 program[42] and were refined on F^2 with SHELXTL (version 6.14).[43] All non-hydrogen atoms were refined anisotropically. Hydrogen atoms were included in calculated positions and were refined using a riding model.

CCDC 875825 and 875826 for the complexes **2a** and **2b** contain the supplementary crystallographic data for this paper. These data can be obtained free of charge from The Cambridge Crystallographic Data Centre via www.ccdc.cam.ac.uk/data_request/cif.

4.2. Biological activity

4.2.1. Reagents

Dimethyl sulfoxide (DMSO) was purchased from Sigma–Aldrich (St. Louis, MO, USA). Cell counting kit-8 (CCK-8) was purchased from DojinDo Laboratories (Kyushu, Japan). Annexin-V FITC and PI reagents were obtained from eBioscience (San Diego, CA, USA). All electrophoresis chemicals were purchased from Bio-Rad Labs (Hercules, CA, USA). Antibodies against cyclin D1, cycling E1 and PCNA were purchased from Epitomics Inc. (Burlingame, CA, USA). Antibody to GAPDH and secondary HRP were purchased from Cell Signaling Technology (Beverly, MA, USA). F-12 K Nutrient Mixture Kaighn's Modification (1X) liquid, RPMI 1640 medium and fetal bovine serum (FBS) were purchased from Gibco Inc. (Grand Island, NY, USA). The human non-small cell lung cancer cell lines A549 and H460 were purchased from the China Cell Bank of SIBS (Shanghai, China). A549 and H460 cells were cultured in F12K and RPMI 1640 medium, respectively, containing 10% heat-inactivated FBS at 37 °C in a humidified atmosphere of 5% CO_2.

4.2.2. In vitro cytotoxicity studies

The cytotoxicity of complexes **2a** and **2b** was evaluated using the CCK-8. In brief, 4 × 10^3 cells (A549 or H460) per well were plated in a 96-well plate and incubated at 37 °C for 18 h. Cells were then treated with the indicated concentrations of complexes **2a** and **2b**, respectively. The plates were incubated at 37 °C for an additional 48 h. Ten microliter of the CCK-8 solution (contains WST-8 [2-(2-methoxy-4-nitrophenyl)-3-(4-nitrophenyl)-5-(2,4-disulfophenyl)-2Htetrazolium, monosodium salt]) was added to each well, and cells were incubated for 2 h. The absorbance was measured using microplate reader (Synergy HT, Bio-Tek) at 450/650 nm as measure reference wavelength, respectively. The average optical density formed in control cells was taken as 100% viability, and the results of treatments were expressed as a percentage of the control. IC_{50} was calculated according to the Log it method.

4.2.3. Detection of apoptosis using Annexin V and PI staining

Cells treated with **2b** for 48 h were harvested by trypsinization, washed twice with ice-cold PBS, then double-stained by Annexin-V FITC and PI according to the instruction of the reagent (eBioscience, SanDiego, CA). The cells in apoptosis were determined by Flow cytometry (FACScan, Becton Dickinson, USA). Cells stained with FITC-Annexin V alone (Annexin V^+/PI^-) were considered in early

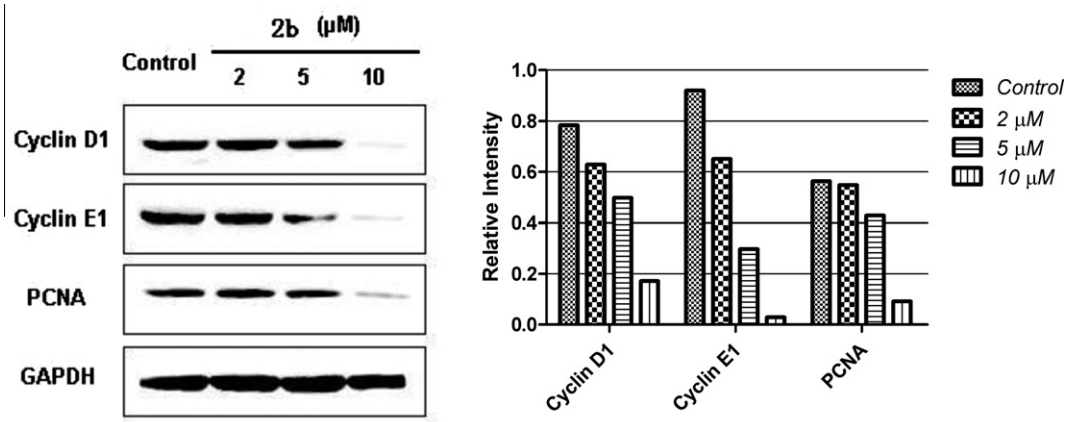

Figure 5. Effects of **2b** on the expression of proteins related to cell cycle progression in A549 human lung cancer cells. Cells were exposed to various concentrations of **2b** for 24 h. The expression levels of cyclin D1, cyclin E1, PCNA and GAPDH were evaluated by Western blot analysis. One of three experiments is presented.

apoptosis, whereas those stained with both FITC-Annexin V and PI (Annexin V^+/PI^+) were considered in the advanced stages of apoptosis or necrosis. The FITC-Annexin V and PI double-negative (Annexin V^-/PI^-) cells were considered alive.

4.2.4. PI staining assay for evaluation of cell cycle distribution

Cell cycle distributions were determined in triplicate using cells grown in 6-well plates (Costar, Cambridge, MA). Cell growth was synchronized in 0.5% FBS medium for 24 h, followed by incubation with different concentrations of **2b** in 10% FBS medium for an additional 48 h. Cells were harvested by trypsinization, then washed twice with ice-cold PBS and fixed by 70% ethanol at 4 °C for at least 2 h. Cells were further washed twice with icecold PBS and stained with 50 μg/ml of PI in the presence of 50 μg/ml RNase A for 30 min at 37 °C. Cell cycle distribution was analyzed by using FACS Calibur (Becton & Dickinson, USA). At least 10,000 cells per sample were collected and analyzed by using the ModFit software.

4.2.5. RNA extraction and real-time quantitative PCR

Total RNA was isolated from 1×10^6 cells treated with **2b** at indicated concentrations and untreated A549 cells by Trizol method. The RNA quantitation was done spectrophotometrically at 260 nm. The integrity and purity of the RNA samples were checked by agarose gel electrophoresis.mRNA levels were measured by real-time quantitative PCR after reverse transcription of RNA. The first-strand cDNA was synthesized from 1 μg total RNA by using oligo dT primers and M-MLV reverse transcriptase in a total reaction volume of 20 μl. The *CCND1*, *CCNE1*, PCNA and β-actin mRNA levels were measured using TaqMan® primers designed using Universal Probe Library Assay Design Center with StepOnePlus™ Real-Time PCR Systems (Applied Biosystems, Foster City, CA, USA).[44] The sequences of the primers are shown in Table 1. PCR reactions were carried out in according to the TaqMan® Master mix PCR kit instructions. The relative expression levels of the target gene were normalized to a house-keeping gene, β-actin, and derived the fold change compared with control, unstimulated cells.

4.2.6. Western blotting

Cells were rinsed twice with ice-cold PBS, and solubilized in lysis buffer containing 50 mM Tris–HCl, pH 7.6, 150 mM NaCl, 1 mM EDTA, 1% (m/v) NP-40, 0.2 mM PMSF, 0.1 mM NaF and 1.0 mM DTT for 30 min on ice. Lysates were centrifuged (15,000 rpm) at 4 °C for 10 min. Protein concentrations were measured using a Bradford assay kit. Equal amounts of the soluble protein were denatured in SDS, electrophoresed on a 10% SDS–polyacrylamide gel, and transferred to PVDF membranes. The PVDF membranes were then blocked for non-specific binding in blocking buffer (5% bovine serum albumin (BSA) in TBST) for 1 h and then washed with TBST 5 times. Subsequently, the membranes were incubated with antibodies at 1:1000 dilutions in antibody dilution buffer (5% BSA in TBST) with gentle shaking at 4 °C overnight and then washed with TBST. After washing, the membranes were exposed to HRP-conjugated secondary antibody at 1:3000 dilutions in antibody dilution buffer for 1 h at the room temperature and then washed again. After six washes with TBST, protein bands were visualized with enhanced chemiluminescence (ECL) Western blotting detection reagents. The ECL image was recorded using the FluorChem Xplor (Alpha Innotech, USA), and the optical density of an equal surface area for each band was determined using Image J software. All blots were stripped and reprobed with polyclonal anti-GAPDH antibody to as certain equal loading of proteins.

4.2.7. Statistical analysis

One-way ANOVA followed by Tukey's Multiple Comparison Testwas performed to determine the statistical significance of differences among groups using GraphPad PRISM version 5.0 software (SanDiego, CA). Differences were considered statistically significant in all experiments at $P < 0.05$. Data are expressed as mean ± -S.E.M. Each experiment was repeated at least three times, and each data point represents the mean of at least three parallel samples.

Table 1
Primers used for real-time quantitative PCR studies in A549 cells

Primer	Sequence	Universal probe number
CCND1	Left-gaagatcgtcgccacctg Right-gacctcctcctcgcacttct	**#67**
CCNE1	Left-ggccaaaatcgacaggac Right-gggtctgcacagactgcat	**#36**
PCNA	Left-tggagaacttggaaatggaaa Right-gaactggttcattcatctctatgg	**#69**
β-actin	Left-ccaaccgcgagaagatga Right-ccagaggcgtacagggatag	**#64**

Acknowledgments

This work was supported by the Scientific Rearch Foundation of Graduate School of Jiangsu Province (CXZZ11_0036), and the Scientific Rearch Foundation of Graduate School of Nanjing University (2010CL04).

References and notes

1. He, J.; Gu, D.; Wu, X.; Reynolds, K.; Duan, X.; Yao, C.; Wang, J.; Chen, C. S.; Chen, J.; Wildman, R. P.; Klag, M. J.; Whelton, P. K. *N. Engl. J. Med.* **2005**, *353*, 1124.
2. http://www.cancer.org/Cancer/LungCancer-Non-SmallCell/DetailedGuide/non-small-cell-lung-cancer-key-statistics; (2012-4-3).
3. Aggarwal, C.; Somaiah, N.; Simon, G. R. *J. Natl. Compr. Canc. Netw.* **2010**, *8*, 822.
4. Malumbres, M.; Barbacid, M. *Nat. Rev. Cancer* **2009**, *9*, 153.
5. Yan, Y. K.; Melchart, M.; Habtemariam, A.; Sadler, P. J. *Chem. Commun. (Camb.)* **2005**, 4764.
6. Gasser, G.; Ott, I.; Metzler-Nolte, N. *J. Med. Chem.* **2011**, *54*, 3.
7. Hartinger, C. G.; Dyson, P. J. *Chem. Soc. Rev.* **2009**, *38*, 391.
8. Suss-Fink, G. *Dalton Trans.* **2010**, *39*, 1673.
9. Chavain, N.; Biot, C. *Curr. Med. Chem.* **2010**, *17*, 2729.
10. Dorcier, A.; Ang, W. H.; Bolano, S.; Gonsalvi, L.; Juillerat-Jeannerat, L.; Laurenczy, G.; Peruzzini, M.; Phillips, A. D.; Zanobini, F.; Dyson, P. J. *Organometallics* **2006**, *25*, 4090.
11. Valliant, J. F.; Guenther, K. J.; King, A. S.; Morel, P.; Schaffer, P.; Sogbein, O. O.; Stephenson, K. A. *Coord. Chem. Rev.* **2002**, *232*, 173.
12. Barth, R. F.; Coderre, J. A.; Vicente, M. G.; Blue, T. E. *Clin. Cancer Res.* **2005**, *11*, 3987.
13. Bregadze, V. I.; Sivaev, I. B.; Glazun, S. A. *Anticancer Agents Med. Chem.* **2006**, *6*, 75.
14. Supuran, C. T.; Scozzafava, A. *Expert Opin. Ther. Patents* **2002**, *12*, 217.
15. Scozzafava, A.; Owa, T.; Mastrolorenzo, A.; Supuran, C. T. *Curr. Med. Chem.* **2003**, *10*, 925.
16. Nomura, M.; Yagisawa, T.; Takayama, C.; Sugiyama, T.; Yokoyama, Y.; Shimizu, K.; Sugimori, A.; Kajitani, M. *J. Organomet. Chem.* **2000**, *611*, 376.
17. Kim, D. H.; Ko, J. J.; Park, K.; Cho, S. G.; Kang, S. O. *Organometallics* **1999**, *18*, 2738.
18. Liu, H. W.; Zhao, Y. S.; Yang, R. Y.; Zheng, M. Q.; Wang, M. Y.; Zhang, X.; Qiu, F.; Wang, H. S.; Zhao, F. *Helv. Chim. Acta* **2010**, *93*, 249.
19. Bao, L.; Wang, M. Y.; Zhao, F.; Zhao, Y. S.; Liu, H. W. *Chem. Biodivers.* **2010**, *7*, 2901.
20. Lakomska, I.; Hoffmann, K.; Topolski, A.; Kloskowski, T.; Drewa, T. *Inorg. Chim. Acta* **2012**, *387*, 455.
21. Chang, T. T.; More, S. V.; Lu, N.; Jhuo, J. W.; Chen, Y. C.; Jao, S. C.; Li, W. S. *Bioorg. Med. Chem.* **2011**, *19*, 4887.
22. Marzano, C.; Sbovata, S. M.; Gandin, V.; Michelin, R. A.; Venzo, A.; Bertani, R.; Seraglia, R. *J. Inorg. Biochem.* **2009**, *103*, 1113.
23. Matesanz, A. I.; Hernandez, C.; Rodriguez, A.; Souza, P. *J. Inorg. Biochem.* **2011**, *105*, 1613.
24. Matesanz, A. I.; Hernandez, C.; Rodriguez, A.; Souza, P. *Dalton Trans.* **2011**, *40*, 5738.
25. Matesanz, A. I.; Joie, C.; Souza, P. *Dalton Trans.* **2010**, *39*, 7059.
26. Skander, M.; Retailleau, P.; Bourrie, B.; Schio, L.; Mailliet, P.; Marinetti, A. *J. Med. Chem.* **2010**, *53*, 2146.
27. Vermes, I.; Haanen, C.; Steffensnakken, H.; Reutelingsperger, C. *J. Immunol. Methods* **1995**, *184*, 39.
28. Sorenson, C. M.; Eastman, A. *Cancer Res.* **1988**, *48*, 6703.
29. Aubry, S.; Pellet-Rostaing, S.; Chabert, J. F. D.; Ducki, S.; Lemaire, M. *Bioorg. Med. Chem. Lett.* **2007**, *17*, 2598.

30. Galluzzi, L.; Morselli, E.; Vitale, I.; Kepp, O.; Senovilla, L.; Criollo, A.; Servant, N.; Paccard, C.; Hupe, P.; Robert, T.; Ripoche, H.; Lazar, V.; Harel-Bellan, A.; Dessen, P.; Barillot, E.; Kroemer, G. *Cancer Res.* **2010**, *70*, 1793.
31. Kazuno, H.; Fujioka, A.; Fukushima, M.; Wataya, Y.; Matsuda, A.; Sasaki, T. *Int. J. Oncol.* **2009**, *34*, 1373.
32. Fu, M. F.; Wang, C. G.; Li, Z. P.; Sakamaki, T.; Pestell, R. G. *Endocrinology* **2004**, *145*, 5439.
33. Wang, C.; Li, Z.; Fu, M.; Bouras, T.; Pestell, R. G. *Cancer Treat. Res.* **2004**, *119*, 217.
34. Schrump, D. S.; Chen, A.; Consoli, U. *Cancer Gene Ther.* **1996**, *3*, 131.
35. Hwang, H. C.; Clurman, B. E. *Oncogene* **2005**, *24*, 2776.
36. Satyanarayana, A.; Kaldis, P. *Oncogene* **2009**, *28*, 2925.
37. Spruck, C. H.; Won, K. A.; Reed, S. I. *Nature* **1999**, *401*, 297.
38. Minella, A. C.; Swanger, J.; Bryant, E.; Welcker, M.; Hwang, H.; Clurman, B. E. *Curr. Biol.* **1817**, *2002*, 12.
39. Thompson, S. L.; Bakhoum, S. F.; Compton, D. A. *Curr. Biol.* **2010**, *20*, R285.
40. Bae, J. Y.; Park, Y. I.; Ko, J.; Park, K. I.; Cho, S. I.; Kang, S. O. *Inorg. Chim. Acta* **1999**, *289*, 141.
41. McElwee-Whitels, L.; Dougherty, D. A. *J. Am. Chem. Soc.* **1984**, *106*, 3466.
42. G.M. Sheldrick, SHELXL-97, Program for the Refinement of Crystal Structures, University of Göttingen, Germany, 1997.
43. Sheldrick, G. M. *Acta Crystallogr. A* **2008**, *64*, 112.
44. https://www.roche-applied-science.com/sis/rtpcr/upl/index.jsp; (2012-4-3).